applied optics

Projector recalibration of three-dimensional profilometry system

PING ZHOU,[1,*] YUNLEI YU,[1] GUOCHAO CAI,[2] AND SHUO HUANG[1,2]

[1]School of Biological Science & Medical Engineering, Southeast University, Nanjing 210096, China
[2]Suzhou Research Institute of Southeast University, Suzhou 215123, China
*Corresponding author: capzhou@163.com

Received 3 December 2015; revised 16 February 2016; accepted 17 February 2016; posted 18 February 2016 (Doc. ID 254342); published 16 March 2016

In three-dimensional profilometry, the primary disadvantage of the monocular system equipped with a projector and a camera is that it is often highly dependent on the projector calibration. The projector calibration errors of the principal point and focal length are analyzed in this paper, and result in measuring the object deviation, including not only the rigid transformation, but also the scale transformation. Unfortunately, the deviation cannot be revealed by reprojection, the normal error analysis method. Here, a systematic recalibration method is proposed to correct the projector calibration errors of the principal point and focal length, where an accurate binocular three-dimensional measurement system is applied. The experimental results show that the method is effective. The three-dimensional measurement accuracy of the monocular system is improved approximately from 1.0 mm before projector recalibration to 0.10 mm afterward.

OCIS codes: (150.0150) Machine vision; (150.1488) Calibration; (120.0120) Instrumentation, measurement, and metrology.

http://dx.doi.org/10.1364/AO.55.002294

1. INTRODUCTION

A three-dimensional measurement system based on structured light has become more and more important in recent decades because of its rapidity, non-contact, and high accuracy. A monocular three-dimensional measurement system is equipped with a camera and a projector. The projector projects a series of encoded patterns onto the object surface and the only camera, which is at an angle to the illumination direction, records the distorted patterns caused by the depth variation of the object surface. As one of the necessary steps, accurate projector calibration is essential for a high-accuracy monocular three-dimensional measurement system. Zhang proposed a plane-based camera calibration method in 2000 [1], which captures at least three checkerboard images to calibrate all the camera's parameters. In Zhang's method, the initial parameters are estimated with the ideal camera model and applied to estimate the final results. The projector calibration method is similar to the camera calibration method. The projector's digital micromirror device (DMD) images are obtained by calculating the checkerboard corners' phase maps in two directions, and the projector is calibrated with these DMD images [2].

Unfortunately, the projector calibration error is many times larger than that of the camera calibration [3–5], so the applications of monocular three-dimensional measurement systems are greatly restricted. One approach proposed to eliminate the projector calibration error is reducing the error of correspondence, such as phase error compensation by using a smoothing spline approximation [6], or adjusting the fringe angle to minimize the phase error [7,8], or a look-up table built to reduce the error of the phase value [9], or introducing ambient light into the phase error model to reduce the gamma effect [10]. Another strategy is to improve the calibration process, including the removal of noise and radial lens distortions during calibration [11], different calibration targets to alter the captured contents [12], an appending laser range finder for optimization constraint [13], and so on. Although there have been many methods to improve the calibration of the projector, and the reprojection error of the projector calibration is almost close to the error of the camera calibration, the measurement error of a monocular system with a single camera is still many times larger than that of a binocular system with two cameras. Therefore, an accurate method to correct the projector calibration is desirable.

In this paper, an alternative method to recalibrate the projector's internal parameters is proposed, based on our discovery that there are residual calibration errors unrevealed by the reprojection error estimation method. The analysis of how the errors affect the reconstruction is given, and the corresponding recalibration method to eliminate the errors is proposed. The experimental results show that the measurement accuracy of the monocular system is improved from 1.0 to 0.1 mm.

The rest of this paper is organized as follows: Section 2 introduces the analysis of the error source of a monocular

three-dimensional measurement system and simulates the results of the analysis. Section 3 discusses the projector recalibration method. Section 4 shows some reconstructed results with recalibrated parameters. Finally, Section 5 concludes this work.

2. PRINCIPLE

A. Monocular System Model

In a monocular three-dimensional measurement system equipped with a camera and a projector, the projector is conceptually regarded as an inverse camera and calibrated through DMD images based on Zhang's method, as explained in the introduction [1]. Assuming Q is an arbitrary point with world coordinates $Q_w = [X_w, Y_w, Z_w]$ in three-dimensional space, Q will be projected onto the real camera image plane and the virtual projector image plane. The relationship between the point Q and its projection on the image sensor can be described as follows, based on a projective model described as Eq. (1):

$$\begin{aligned} v_c &= f_{cx}\frac{r_1X_w + r_2Y_w + r_3Z_w + t_1}{r_7X_w + r_8Y_w + r_9Z_w + t_3} + cc_{cx} \\ u_c &= f_{cy}\frac{r_4X_w + r_5Y_w + r_6Z_w + t_2}{r_7X_w + r_8Y_w + r_9Z_w + t_3} + cc_{cy} \\ v_p &= f_{px}\frac{m_1X_w + m_2Y_w + m_3Z_w + t_4}{m_7X_w + m_8Y_w + m_9Z_w + t_6} + cc_{px}, \end{aligned} \tag{1}$$

where u_c, v_c are the pixel coordinates on the camera imaging plane, and v_p is one of the pixel coordinates on the projector imaging plane, which is found to be a line of corresponding pixels on the DMD image by the phase value at a camera pixel [14]:

$$R_c = \begin{bmatrix} r_1 & r_2 & r_3 \\ r_4 & r_5 & r_6 \\ r_7 & r_8 & r_9 \end{bmatrix} \quad \text{and} \quad T_c = \begin{bmatrix} t_1 \\ t_2 \\ t_3 \end{bmatrix},$$

$$R_p = \begin{bmatrix} m_1 & m_2 & m_3 \\ m_4 & m_5 & m_6 \\ m_7 & m_8 & m_9 \end{bmatrix} \quad \text{and} \quad T_p = \begin{bmatrix} t_4 \\ t_5 \\ t_6 \end{bmatrix},$$

where $[R, T]$ is an extrinsic parameters matrix, which represent a three-by-three rotation matrix and translation vectors between the world coordinate system and the camera/projector coordinate system. A camera or a projector is often described with an intrinsic matrix, including focal length, principal point, pixel skew factor, etc. $[f_{cx}, f_{cy}]$ in Eq. (1) is the focal length along the u- and v-axes of the camera image plane, and $[cc_{cx}, cc_{cy}]$ is the coordinates of the principal point of the camera. The subscripts c and p indicate camera and projector, respectively. Equation (1) represents a linear model of the monocular system. A more elaborate nonlinear model is not discussed to simplify our method. However, the linear model is found to be sufficient to improve the monocular system's accuracy.

Calibration is one of the most important steps of three-dimensional reconstruction. Many methods had been proposed to finish this task; among them, the methods proposed by Zhang and Huang are widely used and applied in our system through projecting horizontal and vertical patterns onto a calibration board [2]. As shown in Fig. 1, compared with their results, a higher calibration accuracy was achieved for projector

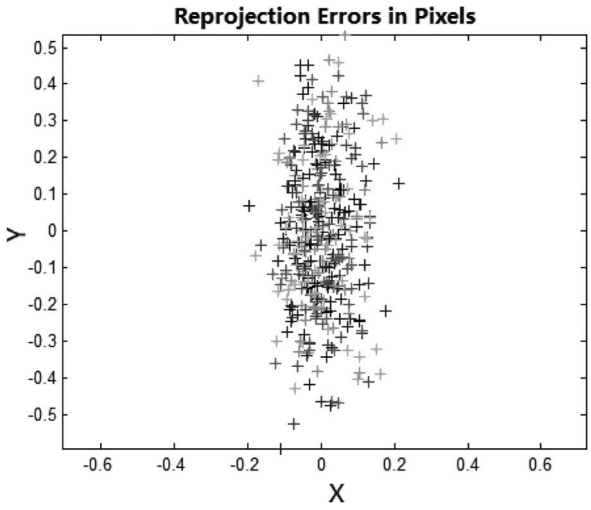

Fig. 1. Reprojection error of projector.

calibration in our system, evaluated with the reprojection method. The reprojection results reveal the error of the control points on the calibration board. There is no doubt that this is a simple and accurate method. It can be seen that most of the reprojection errors are smaller than 0.2 pixels in the X direction and 0.4 pixels in the Y direction. Conceptually, the parameters are very accurate.

However, errors still exist in the process of calibration, which could not be revealed by the reprojection method; thus they will be analyzed and improved with our method, as discussed in the following section.

B. Error Analysis

As discussed in the last section, although the accuracy of the DMD images can be partly verified with the reprojection method, some hidden errors are inevitable. We found that the errors are controlled by the projector's internal parameters. Due to the fact that the projector is designed to project images along the off-axis direction, the principal point and focal length calibrated by the DMD images play an important role in the monocular measurement system's accuracy.

First of all, the error caused by the projector's principal point is analyzed. To simplify the analysis, it is assumed that all parameters in the simulated external and intrinsic matrices are accurate except for one of the components of the projector's principal point, cc_{px}. As shown in Fig. 2, $O_w - X_wY_wZ_w$ is the world coordinate system, $O_c - X_cY_cZ_c$ is the camera coordinate system, and $O_p - X_pY_pZ_p$ is the projector coordinate system. On the projector image plane shown on the right side of Fig. 2, x_p denotes the accurate principle point coordinate, while x_e denotes the inaccurate one acquired by calibration. The difference between x_p and x_e is Δcc. M_l and M_r are two points in three-dimensional space, and the distance from M_l to M_r is L. The rays from M_l and M_r strike the camera and projector image planes represented by the perspective transformation depicted in Eq. (1), as shown in Fig. 2 with the solid line. If the calibration error of the principal point exists, in other words, if cc_{px} in Fig. 2 is x_e instead of x_p, the reconstructed points M_l' and M_r' derived from Eq. (1) will deviate from the original

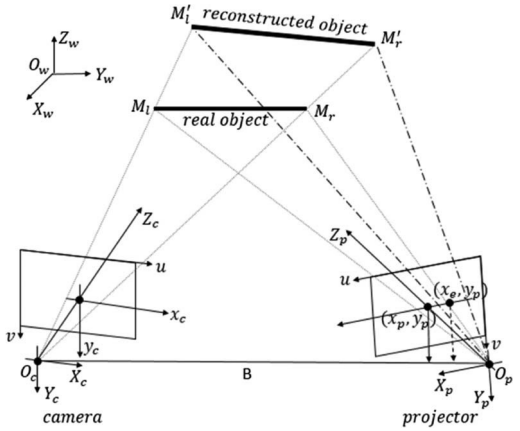

Fig. 2. Error analysis of the principal point.

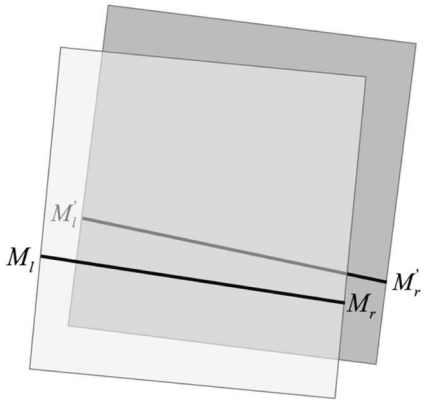

Fig. 3. Actual and reconstructed planes in simulation of principal point.

points M_l and M_r, as shown in Fig. 2. As an example to reveal the quantitative relation of the error and the deviation, here we give an equation, Eq. (2), to describe the error of Z_w, where ΔZ related to the error of cc_{px} and Δcc:

$$Z_w + \Delta Z = \frac{\begin{vmatrix} k_1r_7 - r_1 & k_1r_8 - r_2 & t_1 - k_1t_3 \\ k_2r_7 - r_1 & k_2r_8 - r_2 & t_2 - k_2t_3 \\ k_3m_7 - m_1 & k_3m_8 - m_2 & t_4 - k_3t_6 \end{vmatrix} + \begin{vmatrix} k_1r_7 - r_1 & k_1r_8 - r_2 & t_1 - k_1t_3 \\ k_2r_7 - r_1 & k_2r_8 - r_2 & t_2 - k_2t_3 \\ -\frac{\Delta cc}{f_{px}}m_7 & -\frac{\Delta cc}{f_{px}}m_8 & \frac{\Delta cc}{f_{px}}t_6 \end{vmatrix}}{\begin{vmatrix} k_1r_7 - r_1 & k_1r_8 - r_2 & k_1r_9 - r_3 \\ k_2r_7 - r_1 & k_2r_8 - r_2 & k_2r_9 - r_3 \\ k_3m_7 - m_1 & k_3m_8 - m_2 & k_3m_9 - m_3 \end{vmatrix} + \begin{vmatrix} k_1r_7 - r_1 & k_1r_8 - r_2 & k_1r_9 - r_3 \\ k_2r_7 - r_1 & k_2r_8 - r_2 & k_2r_9 - r_3 \\ -\frac{\Delta cc}{f_{px}}m_7 & -\frac{\Delta cc}{f_{px}}m_8 & -\frac{\Delta cc}{f_{px}}m_9 \end{vmatrix}}, \tag{2}$$

where

$$k_1 = (v_c - cc_{cx})/f_{cx}$$
$$k_2 = (u_c - cc_{cy})/f_{cy}$$
$$k_3 = (v_p - cc_{px})/f_{px}.$$

The reconstructed processing is represented with a dashed line. Although the calibration error of the projector's principal point results in the deviation of three-dimensional points, the deviation is difficult to be revealed by the error analysis method—reprojection. It is worth mentioning that there are not only rigid transformations, including rotation and translation, but also scale transformations that change the actual size of the measured object in three-dimensional measurements. The measurement error derived from the rigid transformations makes no difference to the measurement accuracy; on the contrary, the scale transformation has a significant impact on the measurement accuracy, and has to be corrected.

To verify the analysis validity, point cloud data of a planar board is simulated in Matlab, and a series of parameters of the camera and projector is also generated. x_p is the true value and Δcc is assigned a value of 10 pixels, 1.74% of x_p. As shown in Fig. 3, the light-colored plane is actual, and the dark plane is reconstructed with an inaccurate projector principal point that deviates from the actual plane, as expected in Fig. 2. However, the scale variety is not apparent because Δcc is relatively small in the simulation.

Second, one of the components of the projector's focal length, f_{px} in Eq. (1), is analyzed. A similar assumption is made, except that the focal length is inaccurate. To analyze the measurement error, the actual focal length of the projector, f_{pT}, is expressed as kf_{pe}, while f_{pe} is the inaccurate one acquired by calibration. The reconstructed points M_l' and M_r' derived from Eq. (1) deviate from the original points M_l and M_r, as shown in Fig. 4, where k is greater than 1. It is evident that the line $\overline{M_r'M_l'}$ crosses $\overline{M_rM_l}$ at point M and that there is an angle between these two lines. Particularly, there is a difference between the lengths of $\overline{M_rM_l}$ and $\overline{M_r'M_l'}$, which is the crucial measurement error to be corrected.

Similarly, here we give the error of Z_w, where ΔZ is related to the error of f_{px} and Δf, as described by Eq. (3):

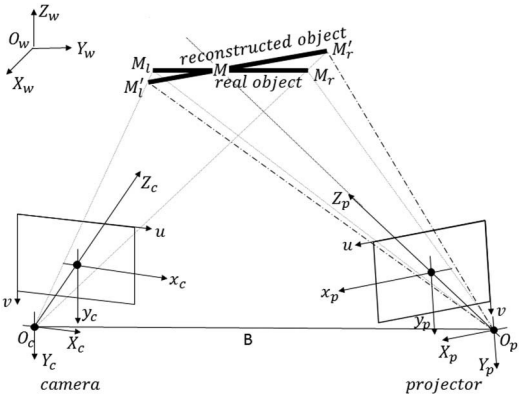

Fig. 4. Error analysis of focal length.

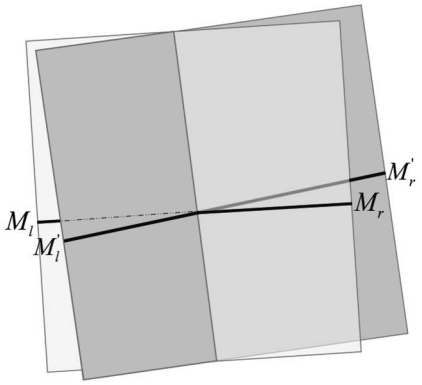

Fig. 5. Actual and reconstructed planes in the simulation of the focal length.

$$X_n = \frac{X_p}{Z_p} = \frac{m_1 X_w + m_2 Y_w + m_3 Z_w + t_4}{m_7 X_w + m_8 Y_w + m_9 Z_w + t_6}. \tag{5}$$

In the traditional projector calibration based on the DMD image, v_p is one of the pixel coordinates on the projector imaging plane acquired by the absolute phase value. Subsequently, the intrinsic parameters cc_{px} and f_{px} are acquired by Zhang's calibration method [1]. Unfortunately, there are inevitable errors in the intrinsic parameters, so the reconstructed point C_w' deviates from C_w. Therefore, a binocular measurement system is introduced in the projector recalibration to capture the actual position of C_w.

A reprojection method is proposed to correct the projector's intrinsic parameters error. In this method, the reprojection column coordinate of the actual position of C_w via

$$Z_w + \Delta Z \approx \frac{\begin{vmatrix} k_1 r_7 - r_1 & k_1 r_8 - r_2 & t_1 - k_1 t_3 \\ k_2 r_7 - r_1 & k_2 r_8 - r_2 & t_2 - k_2 t_3 \\ k_3 m_7 - m_1 & k_3 m_8 - m_2 & t_4 - k_3 t_6 \end{vmatrix} + \begin{vmatrix} k_1 r_7 - r_1 & k_1 r_8 - r_2 & t_1 - k_1 t_3 \\ k_2 r_7 - r_1 & k_2 r_8 - r_2 & t_2 - k_2 t_3 \\ -\frac{\Delta f}{f_{px}} k_3 m_7 & -\frac{\Delta f}{f_{px}} k_3 m_8 & -\frac{\Delta f}{f_{px}} k_3 t_6 \end{vmatrix}}{\begin{vmatrix} k_1 r_7 - r_1 & k_1 r_8 - r_2 & k_1 r_9 - r_3 \\ k_2 r_7 - r_1 & k_2 r_8 - r_2 & k_2 r_9 - r_3 \\ k_3 m_7 - m_1 & k_3 m_8 - m_2 & k_3 m_9 - m_3 \end{vmatrix} + \begin{vmatrix} k_1 r_7 - r_1 & k_1 r_8 - r_2 & k_1 r_9 - r_3 \\ k_2 r_7 - r_1 & k_2 r_8 - r_2 & k_2 r_9 - r_3 \\ -\frac{\Delta f}{f_{px}} k_3 m_7 & -\frac{\Delta f}{f_{px}} k_3 m_8 & -\frac{\Delta f}{f_{px}} k_3 m_9 \end{vmatrix}}. \tag{3}$$

In the simulation of the focal length, the error Δf is assigned a value of 50 pixels, 1.45% of the true value. As shown in Fig. 5, the light-colored plane is actual and the dark one is reconstructed with an inaccurate focal length. It can be seen that the light and dark planes intersect at a line, which is aligned by the points M in Fig. 5. The skew of the intersection line is caused by the angle of view and the skew of projector and camera coordinates relative to the world coordinates. The simulation result proves the analysis convincingly.

In the analysis above, the errors are introduced separately. Actually, the errors always occur simultaneously, and thus should be solved at the same time. The errors of the principal point and that of focal length are independent so that the superposition principle can be applied, which means the errors can be solved simultaneously. The method to solve the errors will be introduced in next section.

3. PROJECTOR RECALIBRATION METHOD

As revealed by the results of the simulation, the errors of the intrinsic parameters cc_{px} and f_{px} really lead to deviations that would not be detected by a monocular measurement system.

In the perspective principle of the projector, assume that $C_w = [X_w, Y_w, Z_w]$ indicates an arbitrary world coordinate in the world coordinates and that $C_p = [X_p, Y_p, Z_p]$ indicates the corresponding world coordinate in the projector coordinates. Then,

$$C_p = R_p C_w + T_p. \tag{4}$$

In addition, we define the normalized coordinate $X_n = (X_p/Z_p)$ as

uncorrected parameters in projector imaging plane is v_F, which is described as

$$v_F = f_{px} X_n + cc_{px}. \tag{6}$$

The reprojection column coordinate of the actual position of C_w via the corrected parameters in the projector imaging plane is v_p as described in Eq. (7), where the corrected parameters are considered to be accurate; thus, v_p can also be obtained by the accurate phase value:

$$v_p = (f_{px} + \Delta f) X_n + cc_{px} + \Delta cc. \tag{7}$$

In Eq. (7), Δf and Δcc are the error of f_{px} and cc_{px}, respectively.

We know that v_p deviates from v_F because for the error of f_{px} and cc_{px}, the deviation is depicted as

$$v_p - v_F = \Delta f X_n + \Delta cc = [X_n \quad 1] \begin{bmatrix} \Delta f \\ \Delta cc \end{bmatrix}. \tag{8}$$

With enough correspondences of v_p from the unwrapped phase map, v_F and X_n from the actual features of the calibration board, Δf and Δcc will be solved according to Eq. (8).

In summary, the projector is recalibrated through the following steps:

(1) Calibration of the monocular system;
(2) Constructing a binocular system by adding a camera to the monocular system;
(3) Calibration of the binocular system;
(4) Reprojecting the calibration board to acquire v_p, v_F, and X_n; and
(5) Solving Eq. (8) with the least-squares method.

4. EXPERIMENTAL RESULTS

To recalibrate the projector's focal length and the principal point in the intrinsic parameters, it is essential to acquire the actual three-dimensional positions of the calibration features, such as the circle centers of the calibration board, as shown in Fig. 6. The circle centers are numbered from 1 to 64, and the nominal distance between adjacent circle centers is 30.00 mm. The monocular measurement system is equipped with an additional camera to form a binocular system, which is accurately calibrated by Zhang's method. Furthermore, the epipolar constraint and multi-frequency heterodyne method are used to acquire the actual three-dimensional positions of the circle centers.

The calibration parameters are expressed as follows: R_{Lc} and R_p are the rotation matrices of the camera and projector of the monocular system, respectively. T_{Lc} and T_p are the corresponding translation vectors. R_{Rc} and T_{Rc} are the rotation matrix and translation vector of the additional camera. KK_p is the projector's intrinsic parameters matrix. Before recalibration, the component cc_{px} of the principal point is 427.2481, and the component f_{px} of the focal length is 1927.9371. The deformation parameters are not expressed in this paper:

$$R_{Lc}=\begin{bmatrix}0.9645 & -0.0418 & 0.2608\\ -0.0493 & -0.9985 & 0.0222\\ 0.2595 & -0.0343 & -0.9651\end{bmatrix} \text{ and } T_{Lc}=\begin{bmatrix}-148.0360\\ -90.5195\\ 937.3280\end{bmatrix},$$

$$R_p=\begin{bmatrix}0.9895 & -0.0449 & 0.1375\\ -0.0791 & -0.9636 & 0.2552\\ 0.1210 & -0.2634 & -0.9571\end{bmatrix} \text{ and } T_p=\begin{bmatrix}-129.9344\\ -243.7679\\ 929.8191\end{bmatrix},$$

$$R_{Rc}=\begin{bmatrix}0.9983 & -0.0499 & -0.0310\\ -0.0490 & -0.9984 & 0.0294\\ -0.0325 & -0.0278 & -0.9991\end{bmatrix} \text{ and } T_{Rc}=\begin{bmatrix}-108.5323\\ -98.0070\\ 976.7139\end{bmatrix},$$

$$KK_p=\begin{bmatrix}1927.9371 & 0 & 427.2481\\ 0 & 1701.1904 & 527.1681\\ 0 & 0 & 1\end{bmatrix}.$$

Subsequently, the projector recalibration results are obtained such that Δcc is 8.9664 and Δf is −6.5563, so that the adjusted value of cc_{px} is 436.2145 and the adjusted value of f_{px} is 1921.3808.

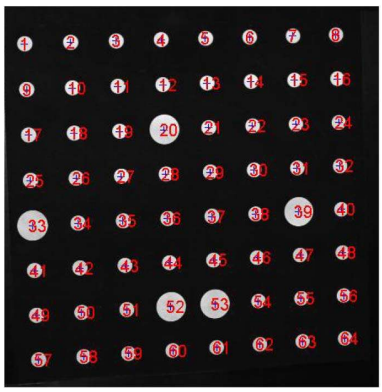

Fig. 6. Calibration board with 64 circle centers.

The three-dimensional positions of the 64 circle centers acquired by the binocular system are considered as actual positions, and two groups of the three-dimensional positions of the 64 circle centers are acquired by the monocular system before and after recalibration. The measurement error of the monocular system is shown in Fig. 7. The Euclidean distance along a circle center before the projector recalibration and the corresponding actual circle center is obtained. Subsequently, the 64 Euclidean distances corresponding to the 64 circle centers before projector recalibration are shown in Fig. 7(a). Furthermore, the similar Euclidean distances after projector recalibration are shown in Fig. 7(b). The maximum Euclidean distance is decreased from 28.75 mm before recalibration to 4.48 mm afterward. The Euclidean distances in Figs. 7(a) and 7(b) indicate that rigid transformations play a leading role in the measurement error not only before projector recalibration, but also after it.

To demonstrate that the scale transformation analyzed in Section 2 is the critical factor in monocular system accuracy, the Euclidean distances between adjacent points on the calibration board are obtained. The errors between the obtained Euclidean distances and the nominal value are shown in Figs. 7(c) and 7(d), and derive from the measurement results before and after projector recalibration, respectively. The asterisk (*) indicates the error of horizontal distance and the cross (+) indicates the error of vertical distance. The maximum errors in Figs. 7(c) and 7(d) are decreased from 1.07 mm before recalibration to 0.26 mm afterward. Eventually, the measurement error is 0.10 mm, and an approximately greater than 80% error is between 0.10 and −0.10 mm.

In addition, a planar board and some complex sculptures are measured before and after the projector is recalibrated. Figure 8 shows the experimental results of the planar board, where the black rectangle and the gray rectangle are acquired by the binocular system and monocular system, respectively. The black rectangle is treated as the true value. The gray rectangle deviates from the actual position before projector recalibration, as shown in Fig. 8(a). However, the surface–surface intersection line depicted in Fig. 5 does not exist in Fig. 8(a), as the deviation rectangle is far from the black rectangle; in other words, the error of the principal point has a major role in this monocular system. The measurement results after projector recalibration are shown in Fig. 8(b). These two rectangles almost coincide, and the intersection line in Fig. 8(b) is very similar to the line in Fig. 5. The measurement error after projector recalibration shows some slight deviation in the lower-right corner and some noise near the intersection line. It may result from both the residual calibration error of the intrinsic parameters matrix and the calibration error of the extrinsic parameters matrix, which is not involved in this work temporarily.

One of the experimental results of complex sculptures is shown in Fig. 9, where the black and gray sculptures are measured by the binocular system and monocular system, respectively, and where the black sculpture shape is considered as the actual one. As shown in Fig. 9(a), there is deviation between the actual shape and measurement shape before projector

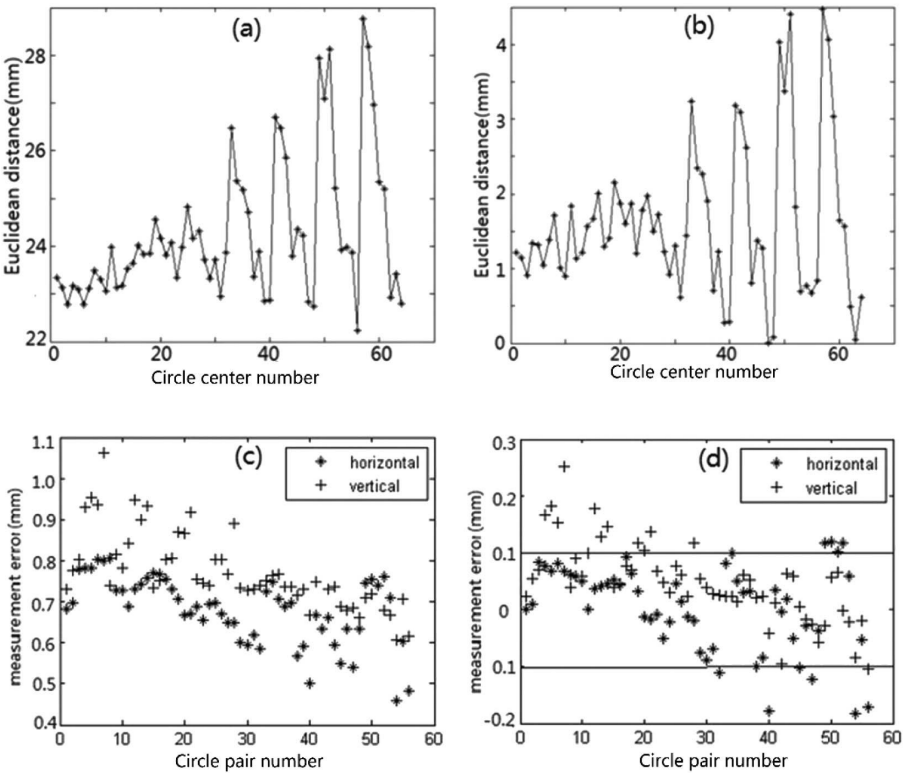

Fig. 7. Measurement results of monocular system before and after recalibration: (a) Euclidean distance between a measured circle center and the corresponding actual one before projector recalibration, (b) corresponding Euclidean distance after projector recalibration, (c) measurement error of adjacent circle centers' Euclidean distances before projector recalibration, and (d) corresponding measurement error after projector recalibration.

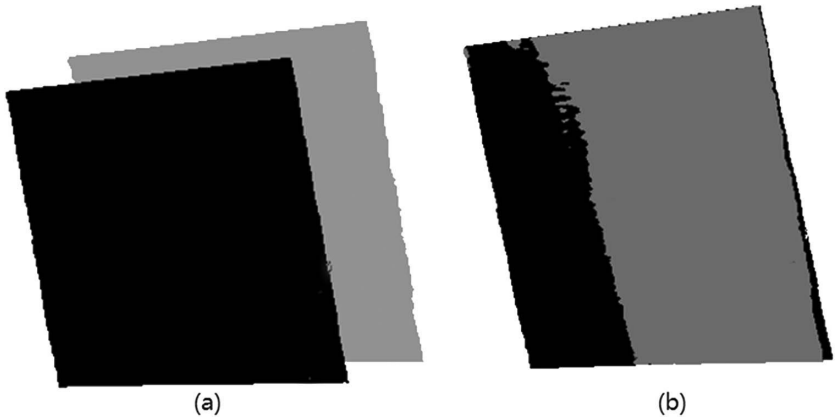

Fig. 8. Comparison of planar board measurement results by the monocular system before and after projector recalibration: (a) actual planar board and reconstructed one with un-recalibrated intrinsic parameters and (b) actual planar board and reconstructed one with recalibrated intrinsic parameters.

recalibration. In comparison with the actual sculpture shape, the reconstructed sculpture shape after projector recalibration is shown in Figs. 9(b) and 9(c) from different angles. The reconstructed sculpture shape acquired by the monocular system is very similar to the actual shape.

These experimental results confirm that the proposed projector recalibration method can successfully improve the accuracy of the monocular three-dimensional measurement system equipped with a camera and a projector. Interestingly, there is a similar problem described in Zhang and Yau's paper [15]: they thought the measurement error was because the mapping is not 100% accurate, and solved it by a rigid transformation method. However, our work in this paper reveals that not only a rigid transformation but also a scale transformation exists in the errors, and the analysis together with the experiments above demonstrates our assumption.

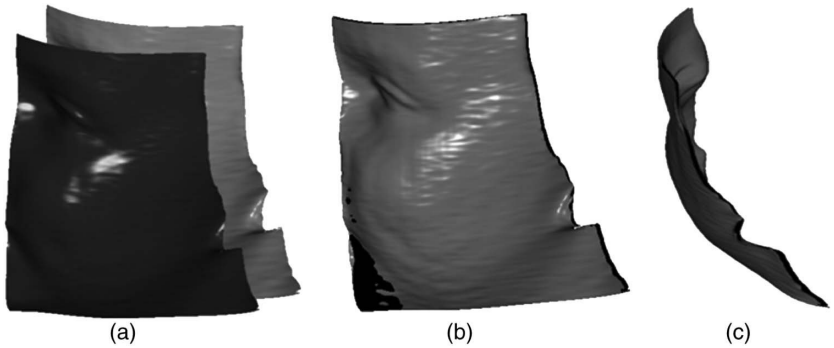

Fig. 9. Comparison between actual and reconstructed sculpture shapes before and after projector recalibration: (a) experimental results before projector recalibration, and (b) and (c) experimental results after projector recalibration from different angles.

5. CONCLUSIONS

System calibration is crucial for any three-dimensional shape measurement system. To improve the accuracy of a monocular three-dimensional measurement system, a projector recalibration method is proposed, as the monocular system accuracy is often highly dependent on the projector calibration. Principally, the measurement errors resulting from the principal point and focal length of the intrinsic parameters matrix are analyzed, while the other intrinsic and extrinsic parameters are ignored in this paper. The experimental results show that the three-dimensional measurement accuracy of monocular system is improved from 1.0 mm before projector recalibration to 0.1 mm afterward.

Funding. National Natural Science Foundation of China (NSFC) (NSFC61127002); Nature Science Foundation of Suzhou (SYG201313).

REFERENCES

1. Z. Y. Zhang, "A flexible new technique for camera calibration," IEEE Trans. Pattern Anal. **22**, 1330–1334 (2000).
2. S. Zhang and P. S. Huang, "Novel method for structured light system calibration," Opt. Eng. **45**, 083601 (2006).
3. Z. Li, Y. Shi, C. Wang, and Y. Wang, "Accurate calibration method for a structured light system," Opt. Eng. **47**, 053604 (2008).
4. X. Chen, J. Xi, J. Ye, and J. Sun, "Accurate calibration for a camera–projector measurement system based on structured light projection," Opt. Lasers Eng. **47**, 310–319 (2009).
5. J. Draréni, S. Roy, and P. Sturm, "Methods for geometrical video projector calibration," Mach. Vis. Appl. **23**, 79–89 (2012).
6. X. Chen, J. Xi, and J. Ye, "Phase error compensation method using smoothing spline approximation for a three-dimensional shape measurement system based on gray-code and phase-shift light projection," Opt. Eng. **47**, 113601 (2008).
7. Y. Wang and S. Zhang, "Optimal fringe angle selection for digital fringe projection technique," Appl. Opt. **52**, 7094–7098 (2013).
8. P. Zhou, X. Liu, and T. Zhu, "Analysis of the relationship between fringe angle and three-dimensional profilometry system sensitivity," Appl. Opt. **53**, 2929–2935 (2014).
9. H. Guo, H. He, and M. Chen, "Gamma correction for digital fringe projection profilometry," Appl. Opt. **43**, 2906–2914 (2004).
10. P. Zhou, X. Liu, Y. He, and T. Zhu, "Phase error analysis and compensation considering ambient light for phase measuring profilometry," Opt. Lasers Eng. **55**, 99–104 (2014).
11. Z. Wang, "Removal of noise and radial lens distortion during calibration of computer vision systems," Opt. Express **23**, 11341–11356 (2015).
12. X. Meng and Z. Hu, "A new easy camera calibration technique based on circular points," Pattern Recogn. **36**, 1155–1164 (2003).
13. Q. Zhang and R. Pless, "Extrinsic calibration of a camera and laser range finder," in *Proceedings of Intelligent Robots and Systems* (IEEE/RSJ, 2004), pp. 2301–2306.
14. K. Zhong, Z. Li, Y. Shi, and Y. Lei, "Fast phase measurement profilometry for arbitrary shape objects without phase unwrapping," Opt. Lasers Eng. **51**, 1213–1222 (2013).
15. S. Zhang and S. T. Yau, "Three-dimensional shape measurement using a structured light system with dual cameras," Opt. Eng. **47**, 013604 (2008).